A New Reference Sample for High Frequency Multipactor Testing

Pablo González, Davide Smacchia, Carlos Alcaide, Pablo Soto, *Member, IEEE,* Ana Rodríguez, Jose Vicente Morro, Rafael Mata, Vicente E. Boria, *Fellow, IEEE,*

***Abstract*—Multipactor is a high-power effect severely limiting the performance of satellite communication links. A reference sample is normally used in the experimental setups for multipactor testing in order to verify its correct operation. However, the low gaps required for high frequencies jeopardize the manufacturability of the devices traditionally used for this purpose. A new reference sample, based on a stepped-impedance resonator, is proposed in this paper. The key design considerations are also outlined. A prototype operating between 17 and 18 GHz has been manufactured and tested, thus proving the novel structure is suitable and advantageous for high frequency bands.**

***Index Terms*—Multipactor, high-power design, microwave filters, transmission lines**

I. Introduction

MULTIPACTOR is an undesired high-power effect occurring in satellite payloads, limiting the maximum transmitted power and the downlink throughput [1], [2]. This key effect is caused by the free electrons inside the device, which after being accelerated by the electromagnetic (EM) field, hit the walls with enough energy to strip secondary electrons from the material surface, thus causing an electron avalanche that eventually leads to a discharge [3]–[5]. Normally it originates between two opposite surfaces separated a distance g referred as the gap [6]–[8]. A multipactor (MP) discharge requires vacuum (so that the particles mean free path is much larger than the gap), materials with a Secondary Emission Yield (SEY) greater than 1 (i.e., providing more than one secondary electron per primary electron impact), and relatively high EM fields (to impact the gap walls with an energy such that the material surface presents an SEY greater than unity) [9], [10].

Recent revisions of multipactor standards admit the use of predictions from modern particle-in-cell simulators or from worst-case curves [11]–[13]. However, the involved margins are so high that MP testing is often required to get space qualification before launching. Multipactor test benches are quite complex, as they involve a large number of components [12], [14]. After a test bed assembly, a reference sample is normally used to check its overall performance and sensitivity. The sample must have a proper frequency-gap product to provide a multipactor threshold (i.e., the lowest power level for which a MP discharge can occur) within the power range of the measurement setup.

In the last decades, the trend is to increase the frequency of operation in satellite communication systems to meet the demands for higher capacity links [15]–[17]. This tendency also posses some challenges in the development of multipactor test samples. In fact, the gap of the reference sample must be reduced to compensate the frequency increase whilst ensuring a relatively low MP threshold. For high frequency bands, however, this can endanger its manufacturability.

This paper proposes a new type of reference sample for high frequency multipactor testing. In Section II the devices traditionally used for this purpose are described, highlighting their limitations for high frequency operation. Next, in Section III a novel reference sample based on a stepped-impedance resonator (SIR) is proposed. A prototype has been designed, manufactured and tested for the operational band ranging from 17 to 18 GHz. The results reported in Section IV reveal the benefits and the validity of the proposed sample.

II. Traditional Multipactor Reference Samples

A. Coaxial cable sample

A coaxial line in vacuum is the compact reference sample normally used for S-band and below [18], [19]. The gap peak voltage, in terms of the mean power P_{in} of a continuous-wave (CW) excitation, is:

$$V = \sqrt{2P_{\text{in}}Z_0} \quad ; \quad Z_0 = \frac{\eta_0}{2\pi}\log\left(\frac{D}{d}\right) \tag{1}$$

where D and d are the diameters of the output and input conductors, respectively, which are fixed to obtain the desired characteristic impedance Z_0 and gap $g = (D-d)/2$. Using Woo's curves for coaxial lines [20], or the ones of Woode and Petit for parallel-plate lines (valid, as a first order approximation, for impedance levels not exceeding 50 Ω) [21], the MP threshold breakdown voltage V_{th} is obtained from the corresponding frequency-gap product. Finally, using (1), an estimation for the multipactor threshold breakdown power level P_{th} of the line can be easily obtained.

This type of sample can be designed to be monomode over a wide frequency range. However, it is difficult to implement narrow gaps to reduce the frequency-gap product,

This work was supported in part by the Ministerio de Ciencia e Innovación (Spanish Government) under R&D project PID2019-103982RB-C41, in part by the European Space Agency (ESA) through several R&D activties, and by the European High Power RF and Space Materials Laboratories of the ESA and Val Space Consortium (VSC) for contributing with its installations - Laboratories co-funded by the European Regional Development Fund.

P. González, C. Alcaide, P. Soto, A. Rodríguez, J. V. Morro and V. E. Boria are with the Instituto de Telecomunicaciones y Aplicaciones Multimedia, Universitat Politècnica de València, 46022 Valencia, Spain (e-mail: pabsopac@dcom.upv.es; vboria@dcom.upv.es).

D. Smacchia and R. Mata are, respectively, with the ESA-VSC European High Power RF Space and Space Materials Laboratories, 46022 Valencia, Spain (e-mail: davide.smacchia@val-space.com).

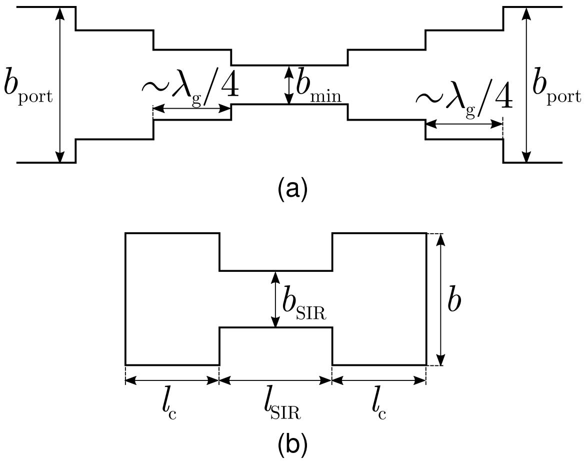

Fig. 1. Side view of a two-step waveguide transformer in (a), and of a short-circuited SIR cavity in (b). Both structures present a uniform width a.

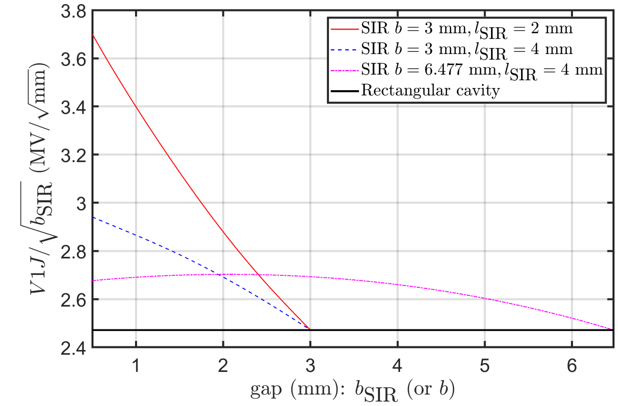

Fig. 2. Normalized critical gap voltage for 1 J of stored energy in a rectangular and SIR cavity of 12.954 mm width and a resonant frequency of 17.5 GHz.

and therefore the multipactor threshold level. Stripline-based transmission lines with input/output coaxial connectors do allow slightly lower gaps, at the expense of higher manufacturing and assembling costs.

B. Waveguide transformer sample

Narrower gaps can be implemented in a rectangular waveguide of reduced height [22], [23]. In order to excite the structure, however, standard rectangular waveguide ports associated to the operational frequency band should be used. Therefore, a stepped transformer is required to transfer the power from the input port to the reduced height rectangular waveguide (i.e., the multipactor critical region), obtaining a parallel-plate like structure as the one shown in Fig. 1a.

For a fundamental mode TE_{10} travelling wave, the peak voltage along the centerline (where the electric field has its maximum amplitude E_0) of a rectangular waveguide of width a and height b can be expressed as:

$$V = |E_0|\,b = 2\sqrt{Z_{\text{TE}_{10}}\frac{b}{a}P_{\text{in}}} \quad ; \quad Z_{\text{TE}_{10}} = \omega\mu/\beta_{10}. \tag{2}$$

For frequency-gap products above 1.5 GHz·mm, the threshold voltage V_{th} for the materials tabulated in the ECSS standard tends to be proportional to $f \times g$ [1], [21], and therefore:

$$P_{\text{th}} = 1\ \text{W} \cdot \left(\frac{V_{\text{th}}}{V_{1\text{W}}}\right)^2 \approx K\frac{(f \times g)^2}{g} \propto f^2 g \tag{3}$$

where K is a proportionality constant and $V_{1\text{W}}$ is the peak voltage for 1 W of mean input power. Expression (3) reveals the increase rate of the multipactor power threshold in terms of both the frequency and the gap height. As gaps of about $0.3 - 0.5$ mm can be accurately manufactured, this type of reference samples are typically used from 4 to 12 GHz.

III. SIR Filter for Multipactor Testing

In order to keep the multipactor threshold within the test bed margins for higher frequency bands, an increase in the $V_{1\text{W}}$ voltage is mandatory. This can be attained by using the EM field accumulation effect that occurs in filter resonators. The threshold power level P_{th} can then be obtained as [19]:

$$P_{\text{th}} = 1\ \text{W} \cdot \left(\frac{V_{\text{th}}}{V_{1\text{W}}}\right)^2 = 1\ \text{W} \cdot \left(\frac{V_{\text{th}}}{V_{1\text{J}}}\right)^2 \cdot \frac{1\text{J}}{TASE_{1\text{W}}} \tag{4}$$

since $V_{1\text{W}} = V_{1\text{J}}\sqrt{TASE_{1\text{W}}/1\ \text{J}}$, being $V_{1\text{J}}$ the critical gap voltage for 1 J of stored energy in its corresponding resonator, and $TASE_{1\text{W}}$ the total time-averaged stored energy (TASE) in such a resonator for a mean input power of 1 W for the whole structure. The $TASE_{1\text{W}}$ can be accurately estimated from the circuit prototype of the filter, whereas $V_{1\text{J}}$ mainly depends on the resonator geometry [1], [19], [24]–[26].

The approach consists on using a filter with a reduced height resonator providing the critical gap. This resonator should be the one with higher $TASE_{1\text{W}}$ in the filter prototype. For a rectangular waveguide cavity of length l with a TE_{10p} resonance, it is straightforward to derive the voltage $V_{1\text{J}}$:

$$TASE = \frac{\epsilon_0}{8}\,|E_0|^2\,abl \quad \rightarrow \quad V_{1\text{J}} = 4\sqrt{\frac{b}{a}\frac{1}{\epsilon_0 p \lambda_{g0}}}. \tag{5}$$

In order to enhance the voltage $V_{1\text{J}}$, however, a more refined solution would be the use of an stepped-impedance resonator (SIR) as the one shown in Fig. 1b, where only the central part of the resonator has a reduced height [27]. It allows a higher EM field concentration in the critical gap, and therefore a lower multipactor power threshold P_{th}. Conversely, it provides a higher gap for a given MP threshold goal, thus simplifying the sample manufacture.

The main design variable in the SIR is the reduced height b_{SIR}. A lower value reduces the multipactor threshold in virtue of (3), but increases the insertion losses (not relevant in this case) and complicates the manufacturability due to the smaller gap and also the reduction of the lengths l_c. Note also that, in order to minimize the effects of the fringing fields (which take electrons out of the critical region and, therefore, increases the MP threshold undesirably), it is advisable that l_{SIR} is higher than $1.5 b_{\text{SIR}}$. Figure 2 compares the normalized voltage $V_{1\text{J}}/\sqrt{b_{\text{SIR}}}$ for a SIR resonator, in terms of b_{SIR}, with the one obtained for a rectangular cavity of the same height.

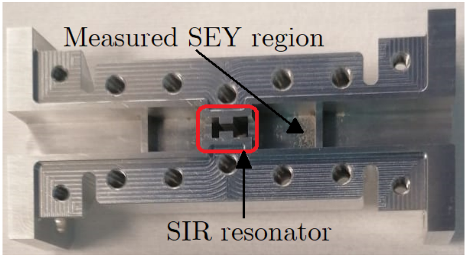

(a)

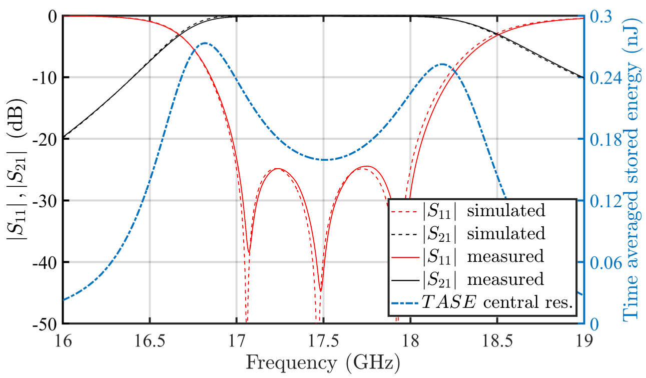

(b)

Fig. 3. One of the two identical half-width parts of the filter, showing the SIR resonator and the region where the SEY was measured, in (a). Comparison between measured and simulated S-parameter response in (b).

The effect of the filter response is accounted for in the parameter $TASE_{1\mathrm{W}}$. As the reference sample should cover a relatively wide bandwidth, this parameter can be increased by using higher order filters, if needed, at the expense of manufacturing costs. Note also that the TASE increases at the edges of the passband, thus allowing a lower MP threshold level than at the filter center frequency. It is worth pointing out that the multipactor test bed imposes a requirement in the minimum return loss level of the sample, which should be about 20 dB or higher.

IV. Results

An in-line third order filter in WR51 rectangular waveguide was designed as a multipactor reference sample covering the frequency range between 17 and 18 GHz. A SIR resonator with $b_{\mathrm{SIR}} = 1.1$ mm and $l_{\mathrm{SIR}} = 2$ mm was used for the central cavity of the filter. The height of the central SIR resonator and its adjacent input and output coupling windows were reduced to 3 mm. This increases $V_{1\mathrm{J}}$, and also the overall length of the resonator to 5.389 mm thus facilitating its manufacture. The iris thickness is set to 1 mm whereas its width is adjusted to synthesize the required coupling value. Figure 3a shows a photograph of the manufactured filter made in bare aluminum.

The measured response is in excellent agreement with the simulated one (see Fig. 3b), proving the good manufacturability of the designed structure. The $TASE_{1\mathrm{W}}$ of the central node of the circuit prototype is also shown in Fig. 3b, with a value of 0.1595 nJ at the passband central frequency, which increases to 0.2374 nJ and 0.2242 nJ at the lower (17 GHz) and upper band-edge (18 GHz), respectively.

TABLE I

Comparison of the predicted multipactor threshold for the different reference samples in WR51 waveguide

	f(GHz)	g(mm)	$V_{1\mathrm{W}}$(V)	Predicted threshold P_{th}	
				Al ECSS	Meas. SEY
SIR filter	17	1.1	56.18	395 W	789 W
	17.5		44.64	668 W	1359 W
	18		51.59	527 W	1055 W
RWG filter	17	1.1	40.95	606 W	1164 W
	17.5		32.32	1055 W	2078 W
	18		36.67	867 W	1734 W
Transformer	17.5	0.55	9.07	2328 W	4156 W
Transformer	17.5	0.2	5.47	727 W	1359 W

Table I compares the CST SPARK3D [28] predictions of the MP threshold for a range of reference samples. Convergence was reached by using 2000 seeding electrons homogeneously distributed in the critical region. Two SEY curves have been considered. The first one is the modified Vaughan SEY model with the parameters of the ECSS standard for aluminum ($\mathrm{SEY}_0 = 0.8$, $\mathrm{E}_1 = 17$ eV, $\mathrm{SEY}_{\max} = 2.92$, $\mathrm{E}_{\max} = 276$ eV), as detailed in [12]. The second one is the SEY measured in the sample surface (see Fig. 3a), attributing the SEY for low impact energies to elastically reflected electrons. The differences between the reference and the measured SEY ($\mathrm{E}_1 \simeq 26$ eV and $\mathrm{SEY}_{\max} \simeq 2.13$) are relevant, causing a variation of about 3 dB in the multipactor predictions. The voltages $V_{1\mathrm{W}}$ have been computed with CST MWS [29] at the center of the critical region, being in good agreement with the theoretical ones. The CST eigenmode solver provided $V_{1\mathrm{J}} = 3.506 \cdot 10^6$ V for the SIR resonator.

It can be observed that a transformer with a central gap of 0.2 mm is required to yield, at the passband center frequency, a MP threshold similar to the one obtained for the filter with a central SIR resonator. This gap is extremely difficult to manufacture, in contrast to the 1.1 mm gap of the SIR filter. On the other hand, the benefit of using the SIR resonator instead of a rectangular cavity of reduced height (RWG filter in Table I) is a reduction of about 2 dB in the MP threshold P_{th}, thus allowing the use of higher gaps to get the same threshold. Note also that the SIR increase of around 3 dB in $V_{1\mathrm{W}}$ translates into a reduction of only 2 dB in P_{th}, due to the higher fringing fields of the SIR resonator in the critical section (which can be reduced by increasing the $l_{\mathrm{SIR}}/b_{\mathrm{SIR}}$ ratio).

The manufactured SIR filter underwent a MP test, obtaining a measured threshold of 1700 W at 17.5 GHz. The discrepancy of 0.97 dB with predictions, which is not unusual, can be attributed to SEY differences (it was not possible to measure the SEY in the critical surfaces, due to the sample geometry), aging effects [30], as well as to inaccuracies of the test bench.

V. Conclusion

A novel reference sample based on a SIR resonator has been proposed for multipactor testing. This sample is able to provide the same MP threshold with a higher gap in the critical region than other types of typical structures used for this purpose. Therefore, it is more suitable for test benches operating at high frequency bands. Measured results from a manufactured sample fully validate the proposed topology.

REFERENCES

[1] M. Yu, "Power-handling capability for RF filters," *IEEE Microw. Mag.*, vol. 8, no. 5, pp. 88–97, Oct. 2007.

[2] R. J. Cameron, C. M. Kudsia, and R. R. Mansour, *Microwave Filters for Communication Systems: Fundamentals, Design, and Applications*, 2nd ed. Hoboken, NJ, USA: Wiley, 2018.

[3] E. W. B. Gill and A. von Engel, "Starting potentials of high-frequency gas discharges at low pressure," *Proc. R. Soc. A*, vol. 192, no. 1030, pp. 446–463, Feb. 1948.

[4] A. J. Hatch and H. B. Williams, "Multipacting modes of high-frequency gaseous breakdown," *Phys. Rev.*, vol. 112, pp. 681–685, Nov. 1958.

[5] J. R. M. Vaughan, "Multipactor," *IEEE Trans. Electron Devices*, vol. 35, no. 7, pp. 1172–1180, Jul. 1988.

[6] R. Kishek, Y.-Y. Lau, L. Ang, A. Valfells, and R. Gilgenbach, "Multipactor discharge on metals and dielectrics: Historical review and recent theories," *Phys. Plasmas*, vol. 5, no. 5, pp. 2120–2126, Apr. 1998.

[7] M. K. Joshi, N. Nayek, T. Tiwari, J. Pidanic, Z. Nemec, and R. Bhattacharjee, "Multiphysics and multipactor analyses of TE_{022}-mode high-power X-band RF window," *IEEE Microw. Wireless Compon. Lett.*, vol. 30, no. 3, pp. 272–274, Mar. 2020.

[8] A. Iqbal, J. Verboncoeur, and P. Zhang, "Two surface multipactor discharge with two-frequency RF fields and space-charge effects," *Phys. Plasmas*, vol. 29, no. 1, p. 012102, Jan. 2022.

[9] J. R. M. Vaughan, "A new formula for secondary emission yield," *IEEE Trans. Electron Devices*, vol. 36, no. 9, pp. 1963–1967, Sep. 1989.

[10] C. Vicente, M. Mattes, D. Wolk, B. Mottet, H. Hartnagel, J. Mosig, and D. Raboso, "Multipactor breakdown prediction in rectangular waveguide based components," in *IEEE MTT-S International Microwave Symposium Digest (IMS)*, Long Beach, CA, USA, June 2005, pp. 1055–1058.

[11] T. P. Graves, "Standard/handbook for multipactor breakdown prevention in spacecraft components," Aeorospace, El Segundo, CA, USA, Tech. Rep. TOR-2014-02198, May 2014.

[12] *Multipaction Design and Test*, European Cooperation for Space Standardization (ECSS) Std. ECSS-E-ST-20-01C, 2020.

[13] *Multipactor Handbook*, European Cooperation for Space Standardization (ECSS) Std. ECSS-E-HB-20-01A, 2020.

[14] O. Monerris, R. Cervera, M. Rodríguez, E. Díaz, C. Alcaide, J. Petit, V. E. Boria, B. Gimeno, and D. Raboso, "High power RF discharge detection technique based on the in-phase and quadrature signals," *IEEE Trans. Microw. Theory Techn.*, vol. 69, no. 12, pp. 5429–5438, Dec. 2021.

[15] J. Christensen. (2012, Aug.) ITU regulation for Ka-band satellite networks. [Online]. Available: https://www.itu.int/md/R12-ITURKA.BAND-C-0001/_page.print

[16] H. Fenech, S. Amos, S. Tomatis, and V. Soumpholphakdy, "High throughput satellite systems: An analytical approach," *IEEE Trans. Aerosp. Electron. Syst.*, vol. 51, no. 1, pp. 192–202, Jan 2015.

[17] O. Kodheli, E. Lagunas, N. Maturo, S. K. Sharma, B. Shankar, J. F. Mendoza, J. C. Merlano, D. Spano, S. Chatzinotas, S. Kisseleff, J. Querol, L. Lei, T. X. Vu, and G. Goussetis, "Satellite communications in the new space era: A survey and future challenges," *IEEE Commun. Surveys Tuts.*, vol. 23, no. 1, pp. 70–109, First quarter 2021.

[18] S. V. Langellotti, N. M. Jordan, Y. Y. Lau, and R. M. Gilgenbach, "CST Particle Studio simulations of coaxial multipactor and comparison with experiments," *IEEE Trans. Plasma Sci.*, vol. 48, no. 6, pp. 1942–1949, Jun. 2020.

[19] P. González, C. Alcaide, R. Cervera, M. Rodríguez, O. Monerris, J. Petit, A. Rodríguez, A. Vidal, J. Vague, J. V. Morro, P. Soto, and V. E. Boria, "Multipactor threshold estimation techniques based on circuit models, electromagnetic fields, and particle simulators," *IEEE Journal of Microwaves*, vol. 2, no. 1, pp. 57–77, Jan. 2022.

[20] R. Woo, "Final report on RF voltage breakdown in coaxial transmission lines," NASA, Jet Propulsion Lab, Pasadena, CA, USA, Tech. Rep. 32-1500, Oct. 1970.

[21] A. Woode and J. Petit, "Diagnostic investigations into the multipactor effect, susceptibility zone measurements and parameters affecting a discharge," ESA, Noordwijk, The Netherlands, Tech. Rep. 1556, Nov. 1989.

[22] A. Berenguer, A. Coves, B. Gimeno, E. Bronchalo, and V. E. Boria, "Experimental study of the multipactor effect in a partially dielectric-loaded rectangular waveguide," *IEEE Microw. Wireless Compon. Lett.*, vol. 29, no. 9, pp. 595–597, Sep. 2019.

[23] W. Cai, T. Huang, C. Bai, Z. Zhao, X. Jin, B. Li, and Z. Yang, "The multipactor simulation and thresholds analysis for an impedance transformer by an improved 3-D PIC method combined with particle merging," *IEEE Trans. Electron Devices*, vol. 69, no. 6, pp. 3419–3426, Jun. 2022.

[24] A. Sivadas, M. Yu, and R. J. Cameron, "A simplified analysis for high power microwave bandpass filter structures," in *IEEE MTT-S International Microwave Symposium Digest (IMS)*, Boston, MA, USA, June 2000, pp. 1771–1774.

[25] C. Ernst, V. Postoyalko, and N. G. Khan, "Relationship between group delay and stored energy in microwave filters," *IEEE Trans. Microw. Theory Techn.*, vol. 49, no. 1, pp. 192–196, Jan. 2001.

[26] C. Wang and K. A. Zaki, "Analysis of power handling capability of microwave filters," in *IEEE MTT-S International Microwave Symposium Digest (IMS)*, Phoenix, AZ, USA, May 2001, pp. 1611–1614.

[27] M. Morelli, I. Hunter, R. Parry, and V. Postoyalko, "Stopband performance improvement of rectangular waveguide filters using stepped-impedance resonators," *IEEE Trans. Microw. Theory Techn.*, vol. 50, no. 7, pp. 1657–1664, Jul. 2002.

[28] SPARK3D 2022. Dassault Systemes. [Online]. Available: https://www.3ds.com/products-services/simulia/products/spark3d

[29] CST Studio Suite 2022. Dassault Systemes. [Online]. Available: https://www.3ds.com/products-services/simulia/products/cst-studio-suite

[30] J. Duran, M. Belhaj, S. Dadouch, J. Sinigaglia, P. Mader, J. Galdeano, and D. Raboso, "Impact of storage conditions and aging effect on RF breakdown and electrical performance in metallic flight hardware," in *Proc. of International Workshop on Multipactor, Corona ans Passive Intermodulation in Space RF Hardware (MULCOPIM)*, Valencia, Spain, Oct. 2022.